Microstructure evolution, texture development, and mechanical properties of hot-rolled 5052 aluminum alloy followed by annealing

Materials Research Express

PAPER

Microstructure evolution, texture development, and mechanical properties of hot-rolled 5052 aluminum alloy followed by annealing

Jianxin Wu[1], **Faramarz Djavanroodi**[2,3], **Ceren Gode**[4], **Mahmoud Ebrahimi**[5] **and Shokouh Attarilar**[6]

[1] Collaborative Innovation Center of Steel Technology, University of Science and Technology Beijing, Beijing, 100083, People's Republic of China
[2] Department of Mechanical Engineering, College of Engineering, Prince Mohammad Bin Fahd University, Al Khobar, Saudi Arabia
[3] Department of Mechanical Engineering, Imperial College London, London, United Kingdom
[4] School of Denizli Vocational Technology, Program of Machine, Pamukkale University, Denizli, Turkey
[5] National Engineering Research Center of Light Alloy Net Forming and Key State Laboratory of Metal Matrix Composites, School of Materials Science and Engineering, Shanghai Jiao Tong University, Shanghai, 200240, People's Republic of China
[6] Key State Laboratory of Metal Matrix Composites, School of Materials Science and Engineering, Shanghai Jiao Tong University, Shanghai, People's Republic of China

E-mail: ebrahimi@maragheh.ac.ir

Keywords: Al-Mg alloys, annealing heat-treatment, TEM observations, texture components, tensile strength, hardness measurement, electrical resistivity

OPEN ACCESS

RECEIVED
10 April 2022

REVISED
25 April 2022

ACCEPTED FOR PUBLICATION
28 April 2022

PUBLISHED
24 May 2022

Abstract

Aluminum alloys, especially the 5000 series, have drawn the attention of the transportation industry due to their lightweight and consequently reduced fuel consumption. In this regard, one of the major problems of this alloy is its low strength and ductility that can be solved using rolling and post-annealing. Accordingly, the present study concentrates on this issue. Microstructural images showed that the rolling process develops a lot of tangled and trapped dislocations in the sample, which gradually lead to the formation of dislocation bundles and networks. Subsequent annealing can produce a more homogeneous structure with clear grain boundaries and low dislocation density in the inner region of the grains. However, grain refinement efficiency through rolling is retained even after annealing. Initial and rolled Al5052 with the maximum intensity of 2.87 and 6.33 possess the lowest and highest overall texture. Also, post-annealing decreases the texture intensity to 6.33 and 4.87 at 150 and 200 °C, respectively. In this context, deformation texture components strengthen considerably after the rolling process due to the formation of shear bands, and they slightly weaken during heat treatment. Although the initial annealing of the as-received material does not cause discontinuous recrystallization during rolling, it may facilitate the material recovery before rolling. Post-annealing was found to decrease the improved effect of strength by rolling and increase the negative influence of ductility due to the inhibition of dislocation strengthening. The results showed that both dislocation density and the precipitation of Mg atoms are influential for electrical resistivity.

1. Introduction

The use of lightweight materials such as aluminum alloys is required in order to reduce the weight of components in the transportation industries for obtaining high fuel efficiency and low air pollution [1]. Amongst various aluminum series, 5000 aluminum alloy as an Al-Mg series alloy has a significant appliance in the military, marine, automobile, aerospace, and other industries due to its suitable weldability and high corrosion resistance. However, the industrial utilization of this non-heat-treatable aluminum series, especially 5052 aluminum alloy (Al5052), is relatively restricted due to its low strength, ductility, formability, and wear resistance. To overcome these limitations, researchers over the last three decades have introduced and examined various techniques such as metal matrix composite (MMC) technologies and plastic deformation processes that improve the microstructure as well as the mechanical properties of the final product [2–6]. Nevertheless, each method has its own pros and cons. For instance, in MMCs, the single material becomes a composite in which the

applied process is most costly. In contrast, processed materials through different plastic deformation techniques, such as conventional metal-forming methods or severe plastic deformation (SPD) are of great significance due to their simplicity and cost-efficiency setup [7–12].

Among them, sheet material processing methods have received a lot of attention from researchers due to their widespread applications in engineering and industry [13]. These methods include rolling [14], deep drawing [15], hydroforming [16], accumulative roll-bonding [17], constrained groove pressing [18], repetitive corrugation and straightening [19], friction stir processing [20], etc [21–23], among which, the continuous techniques are used extensively in the production of metallic sheets and foils. It is worthy to note that more than 70% of metal products are processed through rolling techniques in the world [14, 24]. In this regard, thickness reduction and the following annealing heat treatment are the two most significant parameters during the rolling process. The mentioned post-annealing heat treatment is useful due to the improved formability of the processed sheets. Consequently, it is prominent to evaluate the effects of rolling thickness reduction and post-annealing operation on the microstructure and mechanical properties of the processed materials.

So far, many studies have been carried out on the rolling techniques related to aluminum alloys [25–27]. In this regard, rolling techniques have been developed continuously from the simple to the flexible, strip profile rolling, and eventually accumulative roll-bonding processes [28, 29]. On the other hand, fine-grained and even ultrafine-grained structures have shown significant strength improvement in the aluminum alloys processed by rolling techniques due to the imposed plastic deformation/strains. Wen and Morris found that a decrease in the grain size of the recrystallized Al5182 through cold-rolling followed by annealing led to an increase in both Lüders elongation and serration frequency [30]. Previous studies determined that annealing of cold-rolled continuous cast 5052 and 5182 aluminum alloys resulted in fine equiaxed grains with the cube and R recrystallization textures, while coarse elongated grains of continuous cast 5083 aluminum alloy exhibited a strong M $\{113\}\langle 110\rangle$ texture after complete recrystallization [31, 32]. By investigating the rolling process of Al5052 by Wang *et al* the ultimate tensile strength reached 325 MPa with the low elongation-to-failure at the 87% thickness reduction [33]. Nakamachi *et al* studied the metallurgical design system for optimizing the asymmetric rolling conditions and the tailoring texture to produce a high formability sheet [34]. Cold rolling deformation on powder metallurgy 2024 aluminum alloy was investigated by Wang *et al* [35]. Accordingly, the microstructure gradually evolved from the original equiaxial structure to the fiber one after processing. Yang *et al* indicated that cryogenic rolling of 3003 aluminum alloy could significantly decrease the size of sub-grains and second-phase particles, and increase the dislocation density [36]. The solid-solution treated 2099 aluminum alloy was rolled by Guo *et al* up to a total reduction of 80% at both room and cryogenic temperatures [37]. Accordingly, the nanocrystalline grain structure with a size of 20–100 nm was detectable only in the cryogenic-temperature high-strain rolled sample due to the shear banding behavior. The heat transfer behavior during the hot rolling process of Al7075 was analyzed numerically by Zhao *et al* [38]. It was found that heat transfer between the sheet and roller during the process is a significant factor affecting the temperature distribution of the rolling sheet. The effect of the rolling process followed by natural and artificial aging on the microstructure and mechanical properties of the pre-quenched hot-pressed 2024 aluminum alloy was studied by Krymskiy [39]. The results determined that the cryorolling did not change the type of the initial coarse-fibered microstructure, but produced a well-developed nano cell substructure inside the fibers. During the warm rolling study of 7475 aluminum alloy at 350 °C, it was found that the zirconium element in the alloy led to the stable subgrains with an average diameter of 3 μm after the process and solution heat treatment [40]. An experimental study by Amegadzie and Bishop showed that asymmetric rolled Al6061 has superior tensile properties compared to the symmetric rolled sample [41]. Also, asymmetric rolling reduced the minimum number of passes. In this regard, the Cubic texture $\{100\}\langle 001\rangle$ of the as-received aluminum evolved into shear $\{111\}\langle 110\rangle$ and brass $\{110\}\langle 112\rangle$ texture components after subjecting to the asymmetric and symmetric rolling, respectively.

According to the previous studies, there is no comprehensive investigation of the microstructural and mechanical properties of the hot-rolled and post-annealed 5052 aluminum alloy, which further necessitates this research. Consequently, in this work, it has been attempted to study the effects of rolling thickness reduction and annealing temperature on the microstructure and mechanical behavior of the Al5052.

2. Material and method

For this study, commercially coarse-grained (CG) 5052 aluminum alloy was chosen in the form of a sheet with a thickness, width, and length of 5 mm, 20 mm, and 120 mm, respectively. The nominal compositions of the alloy are listed in table 1 obtained through a full-spectrum direct-reading inductively coupled plasma atomic emission spectroscopy (ICP-AES, Perkin Elmer, Plasma 400). All samples were annealed at 360 °C for 2 h before beginning the process to minimize residual stresses. In this regard, the average grain size of 45 μm with nearly equiaxed grain structure was achieved for the initial sample. The hot-rolling process was performed first on the

Table 1. Chemical composition of the 5052 aluminum alloy (wt.%) used in this study.

Element	Al	Mg	Fe	Si	Cr	Mn	Zn	Cu
Amount	Balance	2.6	0.34	0.24	0.23	0.10	0.10	0.08

prepared sheets with a rolling temperature of 120 °C, roller diameter of 200 mm, and speed of 3 rpm. Accordingly, the imposed cumulative thickness reductions of the processed Al5052 sheet were equal to about 37%, 48%, 57%, and 69%. Then, the deformed sheet with the 57% thickness reduction was conducted by annealing heat treatment at the two annealing temperatures of 150 and 200 °C in the dwell time range of 30–120 min. Eventually, the microstructure characterization and mechanical properties of the initial, hot-rolled, hot-rolled+post-annealed samples at different processing parameters were compared and investigated systematically.

For microstructure characterization and texture evolution, transmission electron microscopy (TEM) and electron backscatter diffraction (EBSD) were applied to the prepared specimens. Accordingly, thin TEM foils were prepared by grinding 1-mm-thick slices down to a thickness of 70–90 μm and thinning them with a double-jet electro-polisher in a solution of 20% $HClNO_4$ and 80% methyl at −15 °C and 24 V. TEM experiments were done through a Philips CM200 microscope operating at 200 kV. Note that the thin foils were tilted to align specimens to the low-index zone axis almost parallel to the incident beam direction to achieve more excellent image contrast. Furthermore, texture measurements were carried out on the initial, rolled, and post-annealed samples using electron backscatter diffraction (EBSD) data. For this aim, the (111), (110), and (100) pole figures were measured and determined. In addition, quantitative texture analysis was performed by calculating the orientation distribution function (ODF) using ATEX software [42].

In addition, tensile specimens were cut in accordance with ASTM E8 along the rolling direction. In this regard, the overall length, gage length, width, width of the grip section, and thickness of the prepared tensile specimens are equal to 110, 50, 10, 18, and 3 mm, respectively, which are parallel to the rolling direction. Uniaxial tensile tests were performed at a cross-head speed of 1 mm min^{-1} on a tensile test instrument equipped with an extensometer with a gauge length of 50 mm. The hardness test was performed in accordance with the ASTM E384 using a UHL VMHT Vickers microhardness tester with 100 g applied load and 10 sec dwell time. Each specimen measurement was carried out three times for the tensile test and eight times for the hardness test, and the related average values were reported. Moreover, the electrical resistivity of the Al5052 sheet under different rolling and annealing conditions was examined. Fisher's Sigmascope was utilized for this purpose. Also, 8 locations were chosen and recorded, and finally, their average value was reported. The electrical resistivity of each material condition was calculated with the following relationship in which R and C are electrical resistivity and electrical conductivity, respectively [30].

$$R\ (\mu\Omega\ \mathrm{cm}) = 172.4/C\ (\%\mathrm{IACS}) \tag{1}$$

3. Results and discussion

Figure 1 shows the microstructure image of the Al5052 sheet after subjecting to the hot-rolling process at four thickness reductions of about 37%, 48%, 57%, and 69%, respectively. Accordingly, it can be inferred that a rolling process develops many tangled dislocations in the sample regardless of the imposed thickness reduction. So, the higher the amount of thickness reduction, the greater the number of dislocations produced, and as a result, qualitatively, its density will increase. Detailed observation in the obtained images indicated the increasing the thickness reduction causes more mobile dislocations to be trapped and entangled in the rolled sample. Subsequently, they lead to the formation of dislocation bundles and ultimately, dislocation networks. Such a mechanism returns to the imposing more further shear plastic strains to the sample with the high thickness reduction. Previous studies [43] determined that higher plastic deformation may balance with the recovery process using the migration of cell walls to fabricate a stabilized low-energy dislocation structure. There are also signs of the production of geometrically necessary dislocations (GNDs) in the produced microstructure. The formation of GNDs is directly related to the rolling thickness reduction in the processed sample.

Figure 2 represents TEM images of hot-rolled Al5052 sheets with a thickness reduction of 57% at different annealing heat-treatment parameters. Note that they were achieved by [100] aluminum zone axis. According to the images obtained at 150 °C annealing temperature, the microstructure of the aluminum sheet contains a high density of dislocations with random entanglement, especially for a low annealing time of 30 or even 60 min In addition, the heterogeneity at the grain boundaries is easily detectable by the presence of numerous distortions. It can be seen that the number of grains with sharp grain boundaries is low, confirming the existence of

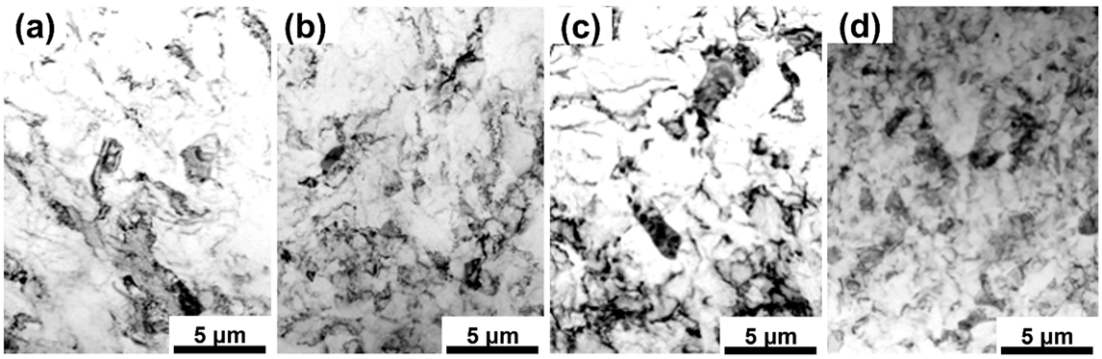

Figure 1. TEM images of the hot-rolled Al5052 with different thickness reductions of (a) 37%, (b) 48%, (c) 57%, and (d) 69%.

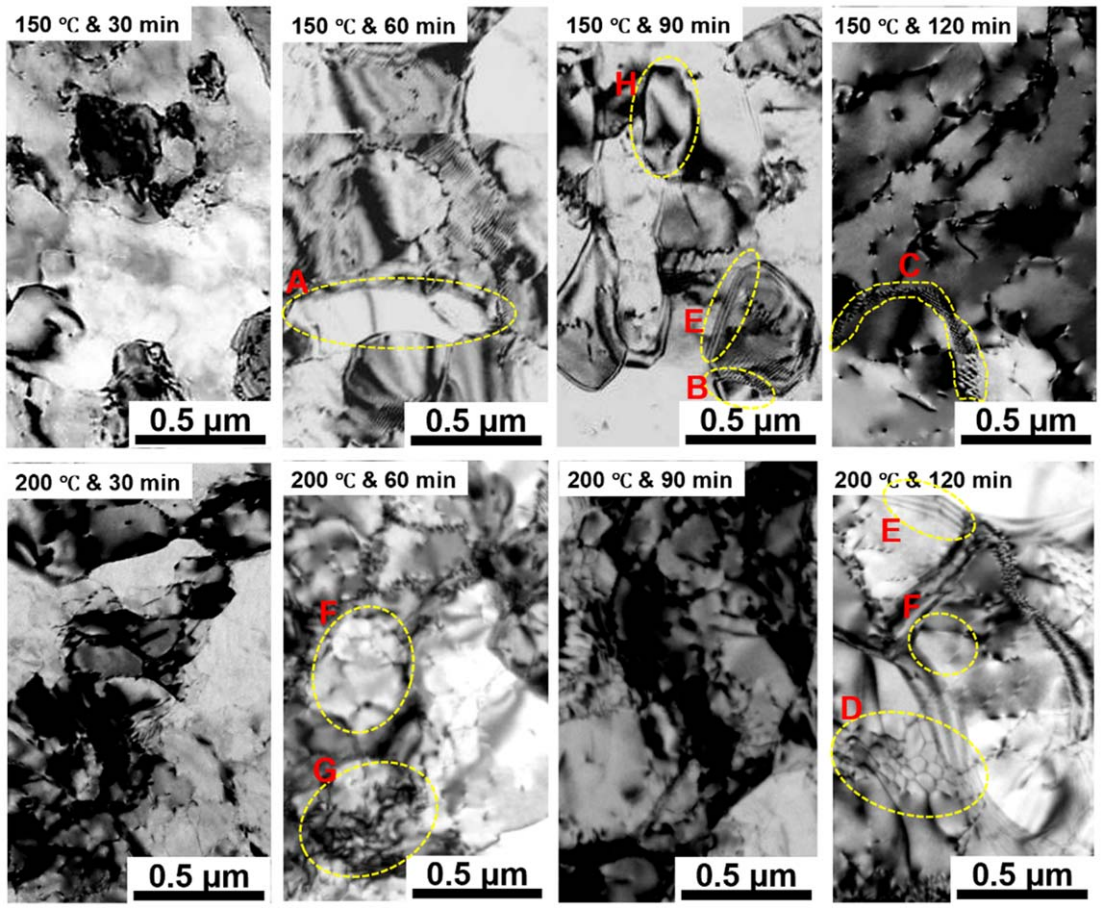

Figure 2. TEM images of the hot-rolled Al5052 sheet with 57% thickness reductions at two annealing temperatures of 150 and 200 °C as well as the dwell time in the range of 30–120 min. Note that regions A, B, C, D, E, F, and G denote elongated grains with subboundaries, polygonal subgrains, tilted grain boundaries, recrystallized grains, distorted grain boundaries, subcell structures, tangled dislocations, and distorted grains, respectively.

considerable density of randomly orientated dislocations, these heterogeneous microstructural features are very common in severely deformed materials [44, 45]. Furthermore, some signs of substructure formation are recognizable. Moreover, the detailed analysis of figure 2 exhibits other microstructural features, such as the existence of elongated grains due to rolling with slight substructure formation as marked by 'A' in the yellow oval. Also, the marked section with 'B' shows the polygonal subgrains that is substituted with the original structure after heat treatment. Region 'C' indicates the tilted grain boundaries, confirming grain boundary impediment effect on dislocations' movement. Stress relaxation due to annealing heat treatment and dislocations' movement along with impeding influence of grain boundaries may lead to formation of these tilted grain boundaries [46]. In the most annealed condition, it is observed the region marked by 'D', showing the

generation of new recrystallized grains without any dislocations. In fact, the previously deformed grains by rolling can be substituted by a new set of defect-free grains that nucleate and grow until the original grains have been consumed entirely. The regions indicated by 'E' displays the distorted grain boundaries and the presence of heterogeneous grain boundaries mainly due to direct effect of deformation. The regions indicated by 'F' shows the formation of subcell structure, subgrains, and activation of restoration mechanisms due to heat treatment. Finally, 'G' displays a region full of dislocation arrays with tangled dislocations which are the clear signs of severe deformation and introduction of many dislocations.

It can be concluded, in general, that more homogeneous structures are achieved with clear grain boundaries and low dislocation density in the inner regions of the grains during the annealing heat treatment. In this context, the areas surrounded by dislocation entanglement in the micrograph are within the range of nano-sized subgrains. It means that obtained grain refinement efficiency by the rolling process is retained even after annealing. By increasing the dwell time of the annealing process to 60–120 min, the number of dislocation tangles and, consequently, the density of dislocations decreases. Therefore, the microstructure of the annealed hot-rolled sheet with the annealing temperature and time of 150 °C and 120 min will have the least number of dislocations. As a result, the subgrain size of the aluminum sample increases to about 750 nm. Such an increase in grain size due to the Hall-Petch relationship decreases the strength of the Al5052 sheet, which will be discussed later. By raising the annealing temperature to 200 °C in a short dwell time, the microstructure of the processed aluminum sheet consists of dense dislocation walls, while the area inside the cells has relatively low dislocations. The subgrain size of the processed sample increases from 700 to 900 nm by increasing the annealing time from 30 to 120 min at an annealing temperature of 200 °C.

The increment of subgrain size due to post-annealing treatment as compared to the rolled condition may attribute to the restoration mechanisms (recovery and static recrystallization) in the processed sample after annealing (softening occurrence). Moreover, during the high-temperature and high-dwell-time annealing operation of the Al5052 sheet processed through high amount of thickness reductions, some grains take part in the static recrystallization mechanism, leading to grain refinement; See figure 2 (200 °C & 120 min). This can be related to the increment of stored energy due to the rolling process that acts as a driving force for the recrystallization occurrence in the rolled sample. As known, the recovery phenomenon leads to the redistribution or/and annihilation of dislocations with/without forming new low angle boundaries, while recrystallization has the capability to annihilate most of the deformation-induced dislocations, forming distortion-free grains with high angle boundaries [47, 48]. It is known that recovery mechanisms rearrange and/or partially annihilate the rolling-induced dense dislocation networks through the dislocations glide and interactions. This phenomenon releases some amount of the previously stored energy due to implemented plastic deformation. Furthermore, recrystallization is progressed mainly by the consumption of surplus volume energy accumulated in the primary rolling process and localized at the stress fields [48–50]. Note that the recrystallization activation energy is typically higher than the recovery occurrence.

Figure 3 shows pole figure on (100), (110), and (111) planes in the Al5052 sheet at the initial state, rolled with 57% thickness reduction, and annealed at the temperatures of 150 and 200 °C with a dwell time of 120 min. In this regard, the initial state of the material has the lowest overall texture, for example, an intensity of 2.87 on the (111) pole figure. By imposing plastic deformation through the rolling process up to 57% thickness reduction, the intensity increases and reaches 6.67 for the mentioned pole figure. Annealing heat treatment leads to the intensity decrease of (111) pole figure to 6.33 and 4.87 in the rolled Al5052 after the applied temperatures of 150 and 200 °C, respectively.

In addition, the significant texture components and the related Miller indices and Euler angles of the rolled FCC metals and alloys during plastic deformation and recrystallization processes are listed in table 2 [29]. Accordingly, figure 4 represents the intensity of each typical texture component in the mentioned conditions of the Al5052 sheets. It should be mentioned that the reported strength for the mentioned texture components was driven by the orientation distribution function (ODF). As can be observed, all mentioned deformation texture components (Copper, Brass, and S) strengthen considerably after the rolling process and weaken thereafter during annealing, irrespective of the applied temperatures. Also, a potential explanation for the stronger deformation components could be due to the formation of shear bands in the microstructure of the rolled Al5052 condition; see figure 1(c). It was reported that Mg atoms in Al-Mg series alloy considerably influence the development of shear and recrystallization textures, assisting the shear banding phenomena in rolling. Rolling reductions and Mg content have a great impact on the shear banding [51]. Moreover, annealing temperatures can significantly affect the recrystallization textures. Shear bands effectively suppress the development of cube recrystallization texture, also high temperature and rapid annealing weaken the cube texture; this is also dependent on the content of Mg atoms. Also, the slight changes in the strength of the recrystallization components (Cube and Goss) indicate that the initial annealing of the as-received material did not lead to the static/dynamic discontinuous recrystallization during the rolling process [52]. However, it may facilitate the recovery phenomenon of the Al5052 sheets before rolling. Furthermore, the post-annealing process has not a

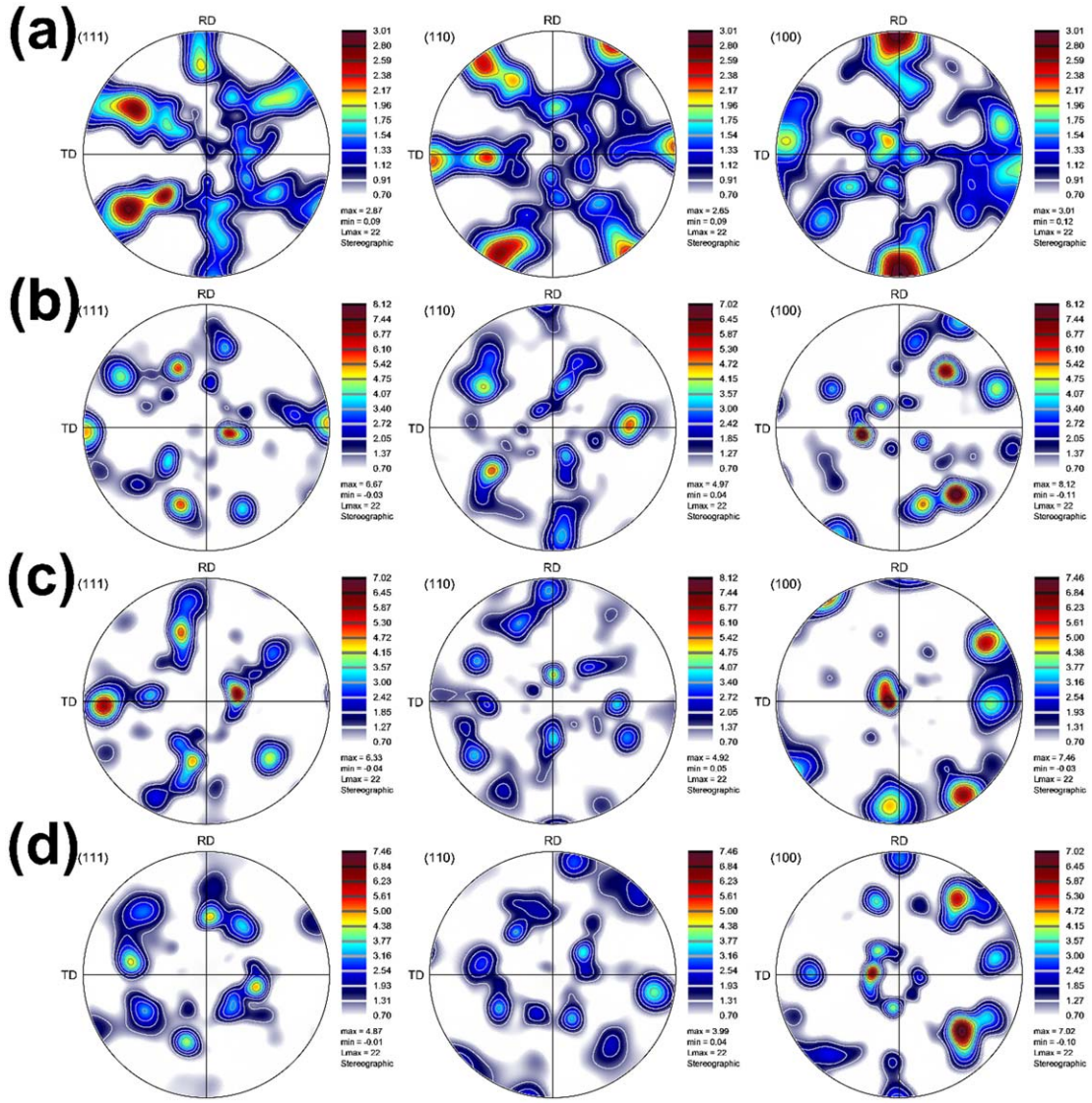

Figure 3. Pole figure of the Al5052 sheets at the (a) initial state and after subjecting to (b) hot-rolled process with 57% thickness reductions and (c) and (d) post-annealing heat treatment at the temperatures of 150 and 200 °C with the dwell time of 120 min, respectively. Note that RD and TD denote rolling and transverse directions, respectively.

Table 2. Important texture components and the relevant Miller indices and Euler angles in the rolled FCC metals and alloys.

		Euler angles		
Component	{hkl} ⟨uvw⟩	φ_1°	Φ°	φ_2°
Copper	{1 1 2} ⟨1 1 1⟩	90	35	45
Brass	{1 1 0} ⟨1 1 2⟩	35	45	0
S	{1 2 3} ⟨6 3 4⟩	59	29	63
Cube	{1 0 0} ⟨0 0 1⟩	0	0	0
Goss	{1 1 0} ⟨0 0 1⟩	0	45	0

considerable effect on the recrystallization texture components. As seen from figure 4, the brass, copper, and S components that are well-known rolling textures of fcc metals with high stacking fault energies are significantly increased during hot rolling and subsequently strongly weaken by annealing in high temperatures. The annealing textures are the combination of the weakened remnant rolling components and the cube texture. As seen, the magnitude of the cube texture is almost the same in all the conditions. This is due to the tendency of cube-oriented grains to be growing rather than reorientation [53]. Moreover, during annealing, the dislocations

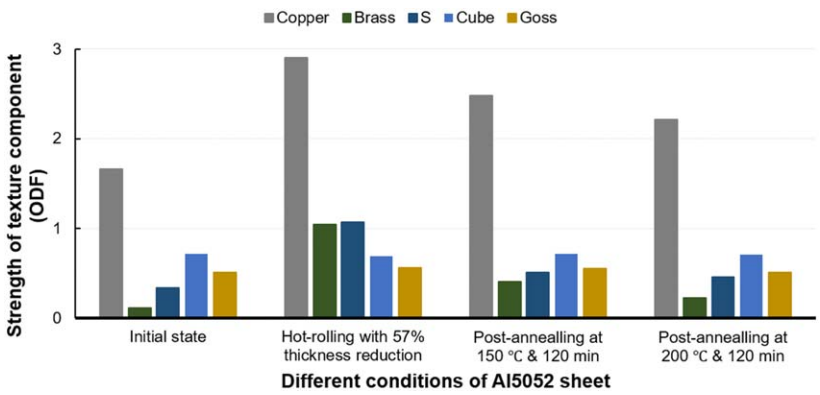

Figure 4. Strength of each typical texture component in terms of orientation distribution function (ODF) for the Al5052 sheets at different conditions of the initial state, hot-rolled process with 57% thickness reductions, and post-annealing heat treatment at the temperatures of 150 and 200 °C with the dwell time of 120 min.

in the grains are actively interacted and annihilated, leading to the considerable drop of recrystallization driving force and intercepting the recrystallization textures [54].

Previous studies [55] revealed that the copper component develops specifically in the layers that are prone to the subgrain formation and shear bands in plastic deformation. It has been shown that the shear bands in homogenously deforming crystals require the single slip activation that decreases the plastic work potential during deformation [56]. Also, the brass component is developed essentially in the adjacent layers of the copper component. Indeed, the planar slip can facilitate the brass component, so this component principally happens adjacent to the copper layers [55, 57]. Moreover, it was found that the Goss component is formed in the brass-oriented grains. This component preferably nucleates in the shear bands and overcomes the brass component [32]. Therefore, the formation of shear bands during the rolling process can facilitate and strengthen the Goss component development. Eventually, the Cube-oriented grains can nucleate at transition bands due to the favored growth relationship with the S component. Consequently, the cube component forms by rotating the copper-oriented grains towards the β fiber in the deformed material [58].

Tensile test and Vickers hardness measurement were carried out on the as-received, hot-rolled at different thickness reductions, and post-annealed heat treatment with various dwell times and temperatures Al5052 sheet. Accordingly, their results in terms of yield strength (YS), ultimate tensile strength (UTS), elongation to failure (El), and average Vickers microhardness (HV) are represented in figure 5. For better understanding and comparison, table 3 lists the mechanical results obtained from the sample under the mentioned conditions in figure 5. As can be observed, the use of the hot-roll process and increase of rolling thickness reduction leads to the improvement of material strength and reduction of ductility. For example, applying a 57% rolling thickness reduction on the Al5052 sheet increases the yield strength by about 70%, ultimate tensile strength by nearly 36%, and hardness by approximately 67%, while the elongation to failure decreases intensely to around 83%. On the other hand, the employment of annealing heat treatment slightly decreases the strength of the material, but elongation to failure significantly improves. According to the microstructure observations, the strength reduction within the annealing process may be related to the inhibition of dislocation strengthening. In addition, the applied temperature has a more significant influence on both strength and ductility of the hot-rolled Al5052 compared to the dwell time. At an annealing dwell time of 60 min, the Al5052 sheet has higher strength (3% in YS and 6% in UTS) and hardness (5%) at the temperature of 150 °C than 200 °C. Also, a 2% difference in strength and a 5% difference in elongation to failure are detectable during the annealing temperature of 150 °C at two dwell times of 90 and 120 min. The results indicated that annealing heat treatment can not diminish the strength and hardness lower than 321 MPa and 74 HV within 150 and 200 °C annealing temperatures and a dwell time of 30–120 min. So, it is rational to conclude that other strengthening mechanisms are involved that can retain the strength of the hot-rolled aluminum during annealing.

As is concluded, the strength and hardness of the rolled sheets are considerably higher than that of the annealed conditions. This is relevant to the three strengthening mechanisms of grain refinement, dislocation, and precipitation; See equation (2). As known, high misorientation grain boundaries ($\geqslant 15°$) may act as an effective dislocation barrier, impeding the movement of mobile dislocations from one crystal to its neighbor. This leads to the enhancement of the material strength during plastic deformation [59, 60]. The finer the grains, the greater the grain boundaries per unit area; as a result, the effect of strengthening will be more evident. The grain boundary strengthening (σ_{gb}) contribution to the yield strength (σ_{yp}) is shown by equation (3) in which k and d are the Hall-Petch constant and average grain size, respectively [61]. In addition, the dislocation

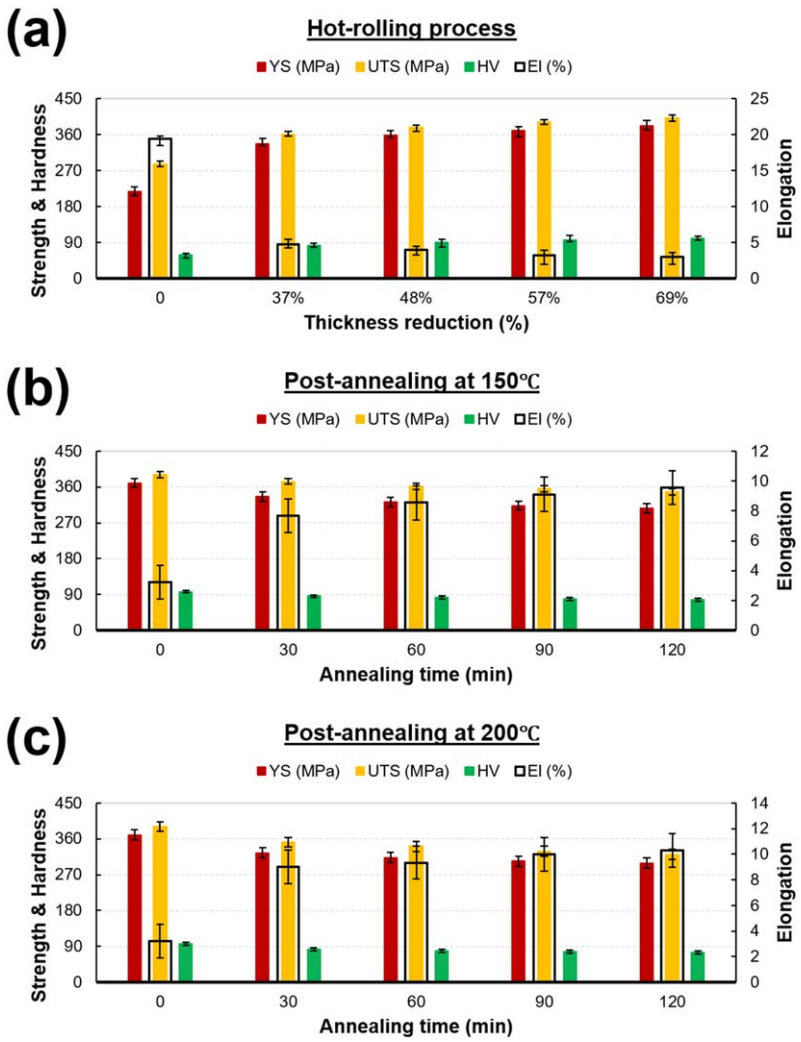

Figure 5. Mechanical properties of Al5052 sheet after subjecting to (a) hot-rolled process with different thickness reductions and (b) and (c) post-annealing heat treatment with different parameters.

Table 3. Tensile and hardness properties of Al5052 sample after rolling process with different thickness reduction as well as post-annealing heat-treatment at two different temperatures of 150 °C and 200 °C and various dwell times.

Material processing condition		Yield strength (MPa)	Ultimate tensile strength (MPa)	Hardness (HV)	Elongation (%)
Initial state	—	218	287	58.2	19.46
Hot-rolled with thickness reduction of	37%	336	361	83.5	4.73
	48%	358	379	91.1	3.95
	57%	370	391	97.2	3.22
	69%	381	402	101.4	2.96
Post-annealing at 150 °C and dwell time of	30 min	336	374	85.8	7.68
	60 min	322	362	83.2	8.55
	90 min	313	356	78.9	9.11
	120 min	306	348	77.4	9.56
Post-annealing at 200 °C and dwell time of	30 min	325	352	83.3	8.99
	60 min	313	341	78.7	9.35
	90 min	304	329	76.3	10.02
	120 min	299	321	73.7	10.31

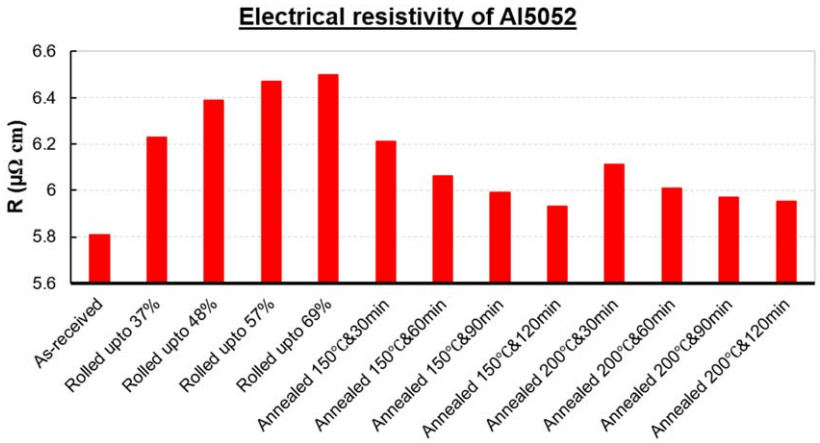

Figure 6. Electrical resistivity of Al5052 sheet after subjecting to hot-rolled process with different thickness reductions of 37%, 48%, 57%, and 69% and the post-annealing heat treatment at two temperatures of 150 and 200 °C in the dwell time range of 30 to 120 min.

strengthening (σ_{dis}) contribution to the yield strength is expressed by equation (4) where M, α, G, b, and ρ represent the Taylor factor, a constant, shear modulus, the Burgers vector, and dislocation density, respectively [36, 62, 63]. The obtained microstructure in figure 1 indicated that the dislocation density gradually increases with the increment of thickness reduction.

$$\sigma_{yp} = \sigma_{gb} + \sigma_{dis} + \sigma_{p} \tag{2}$$

$$\sigma_{gb} = k/\sqrt{d} \tag{3}$$

$$\sigma_{dis} = M\alpha \mathrm{Gb}\sqrt{\rho} \tag{4}$$

$$\sigma_{p} = \frac{0.4MGb}{\pi\lambda\sqrt{1-\upsilon}} \ln\frac{2r}{b} \tag{5}$$

According to the previous studies [64, 65], Mg_2Si and Al_3Fe particles are the second-phase particles in the Al5052, which are incoherent with the Al5052 matrix. In this regard, some dislocation loops encircle the particles after rolling, as can be observed in figure 1. This means that the dislocation glide passes through particles using the Orowan bypass mechanism without shearing them. The incoherent particle strengthening contribution (σ_p) to the yield strength is estimated through the Orowan mechanism; See equation (5). In this relationship, υ and r denote the Poisson ratio and average radius of a circular cross-section in a random plane in a spherical precipitate, respectively. It has been reported that the second-phase particles can be easily broken into smaller particles during deformation processing through the imposed shear stress [66, 67]. Increasing thickness reduction can effectively inhibit the dynamic recovery occurrence. Consequently, it causes the large production of a dislocation density and increases the strength. On the other hand, high shear stress produced during rolling with the high thickness reduction leads to a decrease in the size of the second-phase particles.

Based on the mentioned investigation, the high strength and hardness of the rolled sheets as compared to the annealed ones are principally associated with the contribution of dislocation strengthening and grain-refinement strengthening in the studied Al5052. Moreover, strength and hardness decline with annealing application while the elongation-to-failure improves. This heat treatment decreases the subgrain size and develops the netted dislocation structures with numerous dislocation sources resulting in an improvement of the overall strain-hardening capacity of the alloy [68]. Eventually, texture type can also impact the sample elongation, requiring further investigation [69].

Figure 6 shows the electrical resistivity of the Al5052 sheet subjecting to various rolling and post-annealing parameters. The results indicated that the rolling process considerably increases electrical resistivity while the subsequent heat treatment reduces it moderately. This can be attributed to the dislocation density and precipitation of alloying elements, especially Mg atoms (Mg_2Al_3 compound). In this regard, the previous findings showed that the electrical conductivity varies depending on the lattice d-spacing of the crystallographic planes with a higher peak intensity ratio (I/I_{max}) [6]. Also, dislocations (lattice distortion) around atoms are caused by particles that disrupt the moving path of electrons in an electric field. Therefore, the material conductivity is determined based on the dominant factor in the competition among d-spacing, lattice distortion, and particles transformations.

4. Conclusions

In this study, the influential parameters of rolling thickness reduction as well as post-annealing temperature and dwell time were investigated on the 5052 aluminum alloy. The most notable results of this study are as follows:

- The rolling process developed a lot of tangled dislocations in the sample. Also, increasing the amount of thickness reduction caused more mobile dislocations to be trapped and entangled in the rolled sample, which, in turn, led to the formation of dislocation bundles and networks.
- A more homogeneous structure with clear grain boundaries and low dislocation density in the inner region of the grains was detectable during the annealing of the rolled Al5052. Also, the efficiency of grain refinement in the rolling process was retained even after annealing. Annealing at 150 °C and 120 min decreased dislocation tangles and density. By increasing the temperature to 200 °C, the microstructure consisted of dense dislocation walls with relatively low dislocations of the inside cells. The achieved subgrain size increased from 700 to 900 nm by increasing the dwell time from 30 to 120 min at 200 °C.
- The initial and rolling conditions of the material had the lowest and highest texture intensity with the value of 2.87 and 6.67 on the (111) pole figure, respectively. Annealing treatment decreased it to 6.33 and 4.87 at 150 and 200 °C, respectively. Also, the deformation texture components strengthened considerably after rolling due to the formation of shear bands and weakened thereafter through annealing. The slight changes in the strength of recrystallization components indicated that the initial annealing of the as-received material did not cause the static/dynamic discontinuous recrystallization during rolling. However, it may facilitate the recovery of the Al5052 before rolling.
- The rolling process and increase of thickness reduction led to the improvement of material strength and reduction of ductility. Also, annealing heat treatment slightly decreased the strength due to the inhibition of dislocation strengthening. The highest yield strength, ultimate tensile strength, and hardness belonged to the rolling process of material at a thickness reduction of 69% with the values of 381 MPa, 402 MPa, and 101.4 HV, leading to the lowest elongation of 2.96%. While the most ductile state was attained after post-annealing at 200 °C and 120 min with an elongation of 10.31%. In addition, the applied temperature compared to the dwell time has a more significant influence on both strength and ductility of the rolled Al5052.
- The electrical resistivity of the Al5052 was significantly increased after rolling while the subsequent heat treatment reduced it moderately. The electrical resistivity of the sample was increased from 5.81 to 6.47 $\mu\Omega$.cm through the rolling process at a 57% thickness reduction. However, this resistivity decreased to 5.93 and 5.95 $\mu\Omega$.cm after post-annealing at 150 and 200 °C and the dwell time of 120 min. This was due to the dislocation density and precipitation of alloying elements, especially Mg atoms.
- According to the obtained results, the use of rolling and subsequent annealing operation of Al5052 can improve its strength and formability and reduce the barriers to the utilization of this alloy in the transportation industry, leading to sustainable solutions to increase fuel consumption efficiency. This is an important issue due to global warming, environmental pollution, and the scarcity of fossil fuel resources.

Data availability statement

All data that support the findings of this study are included within the article (and any supplementary files).

Funding

This research received no external funding.

Conflicts of interest

The authors declare no conflicts of interest.

ORCID iDs

Mahmoud Ebrahimi https://orcid.org/0000-0003-2105-9944
Shokouh Attarilar https://orcid.org/0000-0003-3354-9692

References

[1] de la Fuente D 2022 Corrosion of Aluminum, Aluminum Alloys, and Composites *Encyclopedia of Materials: Metals and Alloys* **1** 160–9
[2] Suryanarayana C and Al-Aqeeli N 2013 Mechanically alloyed nanocomposites *Prog. Mater Sci.* **58** 383–502
[3] Ogawa F and Masuda C 2021 Fabrication and the mechanical and physical properties of nanocarbon-reinforced light metal matrix composites: a review and future directions *Mater. Sci. Eng.* A **820** 141542
[4] Zhao Z, Bai P, Du W, Liu B, Pan D, Das R, Liu C and Guo Z 2020 An overview of graphene and its derivatives reinforced metal matrix composites: preparation, properties and applications *Carbon N. Y* **170** 302–26
[5] Samal P, Vundavilli P R, Meher A and Mahapatra M M 2020 Recent progress in aluminum metal matrix composites: a review on processing, mechanical and wear properties *J. Manuf. Process.* **59** 131–52
[6] Jandaghi M R, Pouraliakbar H and Saboori A 2019 Effect of second-phase particles evolution and lattice transformations while ultrafine graining and annealing on the corrosion resistance and electrical conductivity of Al–Mn–Si alloy *Mater. Res. Express* **6** 1065d9
[7] Ebrahimi M and Par M A 2019 Twenty-year uninterrupted endeavor of friction stir processing by focusing on copper and its alloys *J. Alloys Compd.* **781** 1074–90
[8] Figueiredo R B and Langdon T G 2012 Fabricating ultrafine-grained materials through the application of severe plastic deformation: a review of developments in Brazil *J. Mater. Res. Technol.* **1** 55–62
[9] Valiev R Z, Islamgaliev R K and Alexandrov I V 2000 *Bulk Nanostructured Materials from Severe Plastic Deformation* **45** 103–89
[10] Sabirov I, Murashkin M Y and Valiev R Z 2013 Nanostructured aluminium alloys produced by severe plastic deformation: new horizons in development *Mater. Sci. Eng.* A **560** 1–24
[11] Khalaj G, Khalaj M J and Nazari A 2012 Microstructure and hot deformation behavior of AlMg6 alloy produced by equal-channel angular pressing *Mater. Sci. Eng.* A **542** 15–20
[12] Jandaghi M R, Pouraliakbar H, Shiran M K G, Khalaj G and Shirazi M 2016 On the effect of non-isothermal annealing and multi-directional forging on the microstructural evolutions and correlated mechanical and electrical characteristics of hot-deformed Al-Mg alloy *Mater. Sci. Eng.* A **657** 431–40
[13] Gronostajski Z *et al* 2019 Recent development trends in metal forming *Arch. Civ. Mech. Eng.* **19** 898–941
[14] Ikumapayi O M, Akinlabi E T, Onu P and Abolusoro O P 2020 Rolling operation in metal forming: process and principles—a brief study *Mater. Today Proc.* **26** 1644–49
[15] Tiwari P R, Rathore A and Bodkhe M G 2021 Factors affecting the deep drawing process—a review *Mater. Today Proc.* **56** 2902–08
[16] Zhang J, Wang R and Zeng Y 2021 Hydroforming rules and quality control parameters analysis for metal bipolar plate *Eng. Fail. Anal.* **132** 105919
[17] Takata N, Lee S H and Tsuji N 2009 Ultrafine grained copper alloy sheets having both high strength and high electric conductivity *Mater. Lett.* **63** 1757–60
[18] Fan R, Attarilar S, Shamsborhan M, Ebrahimi M, Göde C and Özkavak H V 2020 Enhancing mechanical properties and corrosion performance of AA6063 aluminum alloys through constrained groove pressing technique *Trans. Nonferrous Met. Soc. China* **30** 1790–802
[19] Huang J, Zhu Y T, Alexander D J, Liao X, Lowe T C and Asaro R J 2004 Development of repetitive corrugation and straightening *Mater. Sci. Eng.* A **371** 35–9
[20] Mishra R S, De P S and Kumar N 2014 Friction stir welding and processing *Science and Engineering* (https://doi.org/10.1007/978-3-319-07043-8)
[21] Ebrahimi M 2017 Fatigue behaviors of materials processed by planar twist extrusion *Metall. Mater. Trans. A Phys. Metall. Mater. Sci.* **48** 6126–34
[22] Djavanroodi F, Ebrahimi M and Nayfeh J F 2019 Tribological and mechanical investigation of multi-directional forged nickel *Sci Rep.* **9** 241
[23] Ebrahimi M and Shamsborhan M 2017 Monotonic and dynamic mechanical properties of PTCAE aluminum *J. Alloys Compd.* **705** 28–37
[24] Yu H and Cui X 2022 Rolling forming of multi-scaled metallic foils and sheets *Encycl. Mater. Met. Alloy.* (Amsterdam: Elsevier) 160–81
[25] Zhu H, Ghosh A K and Maruyama K 2006 Effect of cold rolling on microstructure and material properties of 5052 alloy sheet produced by continuous casting *Mater. Sci. Eng.* A **419** 115–21
[26] Yu H and Cui X 2022 Rolling Forming of Multi-Scaled Metallic Foils and Sheets *Encyclopedia of Materials: Metals and Alloys* **4** 160–81
[27] Engler O and Knarbakk K 2021 Temper rolling to control texture and earing in aluminium alloy AA 5050A *J. Mater. Process. Technol.* **288** 116910
[28] Engler O, Schäfer C, Brinkman H J, Brecht J, Beiter P and Nijhof K 2016 Flexible rolling of aluminium alloy sheet—process optimization and control of materials properties *J. Mater. Process. Technol.* **229** 139–48
[29] Roy S, Satyaveer Singh D, Suwas S, Kumar S and Chattopadhyay K 2011 Microstructure and texture evolution during accumulative roll bonding of aluminium alloy AA5086 *Mater. Sci. Eng.* A **528** 8469–78
[30] Wen W and Morris J G 2004 The effect of cold rolling and annealing on the serrated yielding phenomenon of AA5182 aluminum alloy *Mater. Sci. Eng.* A **373** 204–16
[31] Xia S L, Ma M, Zhang J X, Wang W X and Liu W C 2014 Effect of heating rate on the microstructure, texture and tensile properties of continuous cast AA 5083 aluminum alloy *Mater. Sci. Eng.* A **609** 168–76
[32] Li J, Liu W C, Zhai T and Kenik E A 2005 Comparison of recrystallization texture in cold-rolled continuous cast AA5083 and 5182 aluminum alloys *Scr. Mater.* **52** 163–8
[33] Wang B, Chen X H, Pan F S, Mao J J and Fang Y 2015 Effects of cold rolling and heat treatment on microstructure and mechanical properties of AA 5052 aluminum alloy *Trans. Nonferrous Met. Soc. China (English Ed.)* **25** 2481–9
[34] Nakamachi E, Kuramae H, Sakamoto H and Morimoto H 2010 Process metallurgy design of aluminum alloy sheet rolling by using two-scale finite element analysis and optimization algorithm *Int. J. Mech. Sci.* **52** 146–57
[35] Wang T, Huang Y, Ma Y, Wu L, Yan H, Liu C, Liu Y, Liu B and Liu W 2021 Microstructure and mechanical properties of powder metallurgy 2024 aluminum alloy during cold rolling *J. Mater. Res. Technol.* **15** 3337–48
[36] Yang Q Y, Zhou Y L, Tan Y B, Xiang S, Ma M and Zhao F 2021 Effects of microstructure, texture evolution and strengthening mechanisms on mechanical properties of 3003 aluminum alloy during cryogenic rolling *J. Alloys Compd.* **884** 161135
[37] Guo F, Dong H, Huang W, Yang X, Hu L, Li M and Jiang L 2021 Nanocrystalline structure fabricated by cryogenic temperature rolling of AA 2099 aluminum alloy *J. Alloys Compd.* **864** 158293
[38] Zhao X, Chen L, He K, Wu N and Zeng J 2019 Effect of contact heat transfer on hot rolling of aluminum alloy *Procedia Manuf.* **37** 91–6

[39] Krymskiy S, Sitdikov O, Avtokratova E and Markushev M 2020 Aluminum alloy ultrahigh-strength sheet due to two-level nanostructuring under cryorolling and heat treatment *Trans. Nonferrous Met. Soc. China (English Ed.* **30** 14–26
[40] Tanaka H and Minoda T 2014 Mechanical properties of 7475 aluminum alloy sheets with fine subgrain structure by warm rolling *Trans. Nonferrous Met. Soc. China (English Ed.* **24** 2187–95
[41] Amegadzie M Y and Bishop D P 2020 Effect of asymmetric rolling on the microstructure and mechanical properties of wrought 6061 aluminum *Mater. Today Commun.* **25** 101283
[42] Beausir B and Fundenberger J-J (2017) Analysis Tools for Electron and X-Ray DiffractionATEX - software, Univ. Lorraine - Metz (www.atex-software.eu)
[43] Attarilar S, Ebrahimi M, Hsieh T-H, Uan J-Y and Göde C 2021 An insight into the vibration-assisted rolling of AA5052 aluminum alloy: tensile strength, deformation microstructure, and texture evolution *Mater. Sci. Eng.* A **803** 140489
[44] Attarilar S, Salehi M T and Djavanroodi F 2019 Microhardness evolution of pure titanium deformed by equal channel angular extrusion *Metall. Res. Technol.* **116** 408
[45] Attarilar S, Djavanroodi F, Ebrahimi M, Al-Fadhalah K J, Wang L and Mozafari M 2021 Hierarchical microstructure tailoring of pure titanium for enhancing cellular response at tissue-implant interface *J. Biomed. Nanotechnol.* **17** 115–30
[46] Kondo S, Mitsuma T, Shibata N and Ikuhara Y 2016 Direct observation of individual dislocation interaction processes with grain boundaries *Sci. Adv.* **2** 1501926
[47] Heidarzadeh A *et al* 2020 Friction stir welding/processing of metals and alloys: a comprehensive review on microstructural evolution *Prog. Mater Sci.* **117** 100752
[48] Alaneme K K and Okotete E A 2019 Recrystallization mechanisms and microstructure development in emerging metallic materials: a review *J. Sci. Adv. Mater. Devices.* **4** 19–33
[49] Huang K and Logé R E 2016 A review of dynamic recrystallization phenomena in metallic materials *Mater. Des.* **111** 548–74
[50] Rollett A, Humphreys F, Rohrer G S and Hatherly M 2004 *Recrystallization and Related Annealing Phenomena* 2nd edn
[51] Koizumi M and Inagaki H 1999 Role of shear band in texture control of Al-Mg alloys *Met. Mater.* **5** 511–17
[52] Zhang L, Wang Y, Yang X, Li K, Ni S, Du Y and Song M 2017 Texture, microstructure and mechanical properties of 6111 aluminum alloy subject to rolling deformation *Mater. Res.* **20** 1360–68
[53] Lee J-K and Lee D N 2008 Texture control and grain refinement of AA1050 Al alloy sheets by asymmetric rolling *Int. J. Mech. Sci.* **50** 869–87
[54] Lee S H and Lee D N 2001 Analysis of deformation textures of asymmetrically rolled steel sheets *Int. J. Mech. Sci.* **43** 1997–2015
[55] Ray R K 1995 Rolling textures of pure nickel, nickel-iron and nickel-cobalt alloys *Acta Metall. Mater.* **43** 3861–72
[56] Wagner P, Engler O and Lücke K 1995 Formation of Cu-type shear bands and their influence on deformation and texture of rolled f.c.c. {112} ⟨111⟩ single crystals *Acta Metall. Mater.* **43** 3799–812
[57] Ortiz M and Repetto E A 1999 Nonconvex energy minimization and dislocation structures in ductile single crystals *J. Mech. Phys. Solids* **47** 397–462
[58] Engler O, Vatne H E and Nes E 1996 The roles of oriented nucleation and oriented growth on recrystallization textures in commercial purity aluminium *Mater. Sci. Eng.* A **205** 187–98
[59] Kamikawa N, Huang X, Tsuji N and Hansen N 2009 Strengthening mechanisms in nanostructured high-purity aluminium deformed to high strain and annealed *Acta Mater.* **57** 4198–208
[60] Liu Y, Zhao X, Li J, Bhatta L, Luo K, Kong C and Yu H 2021 Mechanical properties of rolled and aged AA6061 sheets at room-temperature and cryogenic environments *J. Alloys Compd.* **860** 158449
[61] Zuiko I S, Mironov S and Kaibyshev R 2019 Microstructural evolution and strengthening mechanisms operating during cryogenic rolling of solutionized Al-Cu-Mg alloy *Mater. Sci. Eng.* A **745** 82–9
[62] Zherebtsov S V, Dyakonov G S, Salem A A, Sokolenko V I, Salishchev G A and Semiatin S L 2013 Formation of nanostructures in commercial-purity titanium via cryorolling *Acta Mater.* **61** 1167–78
[63] Ma K, Wen H, Hu T, Topping T D, Isheim D, Seidman D N, Lavernia E J and Schoenung J M 2014 Mechanical behavior and strengthening mechanisms in ultrafine grain precipitation-strengthened aluminum alloy *Acta Mater.* **62** 141–55
[64] Li Y J, Muggerud A M F, Olsen A and Furu T 2012 Precipitation of partially coherent α-Al(Mn,Fe)Si dispersoids and their strengthening effect in AA 3003 alloy *Acta Mater.* **60** 1004–14
[65] Long L, Pan Q, Li M, Ye J, Sun Y, Wang W, Luo Y, Li X, Peng Z and Liu S 2020 Study on microstructure and mechanical properties of 3003 alloys with scandium and copper addition *Vacuum* **173** 109112
[66] He H, Yi Y, Huang S and Zhang Y 2018 Effects of cold predeformation on dissolution of second-phase Al2Cu particles during solution treatment of 2219 Al-Cu alloy forgings *Mater. Charact.* **135** 18–24
[67] Dong F, Yi Y, Huang C and Huang S 2020 Influence of cryogenic deformation on second-phase particles, grain structure, and mechanical properties of Al–Cu–Mn alloy *J. Alloys Compd.* **827** 154300
[68] Cheng W, Liu W and Yuan S 2019 Deformation behavior of Al–Cu–Mn alloy sheets under biaxial stress at cryogenic temperatures *Mater. Sci. Eng.* A **759** 357–67
[69] Yoshida K, Ishizaka T, Kuroda M and Ikawa S 2007 The effects of texture on formability of aluminum alloy sheets *Acta Mater.* **55** 4499–506